



INDIRECT SELF TUNING ADAPTIVE CONTROL OF DOUBLE STARS INDUCTION MACHINE BY SLIDING MODE

HADJI CHAABANE¹, KHODJA DJALAL EDDINE², CHAKROUNE SALIM¹

Key words: Double star induction machine (DSIM), Sliding mode control (SMC), Indirect self tuning control, RST regulator.

In this paper we will establish a sliding mode adaptive control based on the direct rotor field control applied to the double stars induction machine. Due to the performance limitations of conventional controllers due to their sensitivities, non-linearity and parametric variations, the indirect "self tuning" adaptive control is applied. Indeed, the recursive least squares algorithm is used to obtain the identification model in order to adapt the RST regulator (three-branched structure regulator) parameters in real time, and then generate the control law. However, the location of the sliding mode regulators to the control chain by indirect rotor flow orientation offers good static and dynamic performance, and almost total rejection of the disturbance. Finally, all the results obtained showed the robustness of the control in front of the variation of the parameters of the system and load.

1. INTRODUCTION

Modern variable speed drive technology is based on the increasing use of the dual stator asynchronous machine due to its robustness, electromechanical reliability and low cost [1]. In addition, the supply of asynchronous machines with double stator voltage inverters causes currents harmonics which adds additional losses. Their control becomes an economic issue [2]. Indeed, it is important to control this type of machine taking into account the variation of the parameters (because of the environment) which can hinder their operation.

Modern control techniques lead to control of asynchronous machines comparable to that of the dc machine. These techniques include direct torque control, state feedback control, vector control, and adaptive control. These techniques use both conventional and modern regulators that make the previously mentioned controls robust. By way of example, the fuzzy regulator has been proposed in [3], for sliding surface adjustment of a regulator by sliding mode which guarantees to give a certain robustness. The results obtained in simulation show that the performances are much better than the one obtained with a sliding mode, the fuzzy logic knew a real success in the control of the asynchronous machines double star. In addition, the sliding mode control presented in [3, 4] has been used for the variable speed drive of the double star asynchronous machine. The control thus constructed makes it possible to ensure, in addition to good tracking performance, a fast dynamic and a short response time. However, this control law represents some disadvantages that can be summarized in three points.

The first is the need to have accurate information on the evolution of the system in the state space and the upper bounds of the uncertainties of the sliding surfaces and the disturbances of the load. The second disadvantage lies in the phenomenon of continuation in case of application of a load torque; this situation makes it possible to have a static error in the response of the speed [5, 6]. The third disadvantage lies in the use of the switching function in the control law to ensure the passage of the approach phase to that of the slip. This gives rise to the phenomenon of

chattering, which consists of sudden and rapid changes in the control signal [6, 7].

To remedy these problems, several approaches have been presented in the literature, twisting, super twisting [8–10]. Indeed, for the first disadvantage several works have been focused on the combination of sliding modes with adaptive control as an effective solution [11–13].

At present adaptive control is of great importance in the control domain, this control is dominant in systems with uncertainties, structural disturbances and environmental variations. The main object of adaptive control is the synthesis of adaptation law, in order to automatically adjust loop controllers in real time. This is to achieve or maintain a certain level of performance when the process parameters to be controlled are difficult to determine or vary over time. In fact, the interest of the adaptive control appears essentially at the level of parametric perturbations that is to say on the characteristics of the process to be controlled. These disturbances affect the variables to be regulated or controlled. In addition, the RST polynomial controller can improve the performance of the dual-star induction machine in terms of overshoot, speed, interference cancellation and ability to maintain high performance [4–14].

In this paper, Section 2 is devoted to adaptive self-tuning control as part of adaptive control methods. Section 3 will be devoted to the calculation of RST parameters by pole placement, then the use of RST for the sliding mode of the DSIM. Finally, in Section 4, we will present the results of the simulation of the robustness test of this command in front of the change of parameters.

2. INDIRECT SELF TUNING ADAPTIVE CONTROL

The synthesis of a self tuning speed controller usually imposes two phases namely; first, define a discrete linear model that translates the input-output relationship of the system (vector control + inverter + DSIM machine), therefore, establish via the identification techniques a model that relates the variations of the reference torque to the variations of speed. of DSIM. Secondly, exploit this model established in a control loop based on an adaptive RST regulator which aims to enslave the DSIM output speed on the reference speed, whatever the disturbances and

^{1,2} Research Laboratory on the Electrical Engineering, Faculty of Technology, University of M'Sila, BP 166, Ichbilia 28000, Algeria, E-mails: chaabane.hadji@univ-msila.dz, salim.chakroune@univ-msila.dz.

² Signals & Systems Lab, Institute of Electrical and Electronic Engineering, Boumerdes, Algeria, E-mail: djalaeddine.khodja@univ-msila.dz

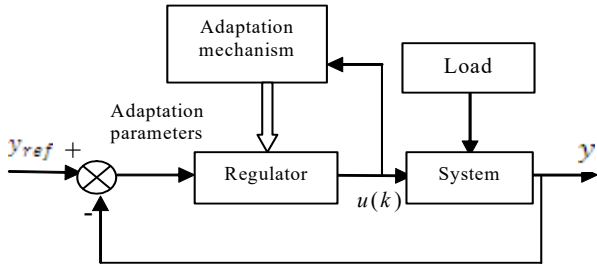


Fig. 1 – Self tuning adaptive control principle diagram.

the parametric variations, as indicated in Fig. 1.

2.1. PRINCIPLE OF PARAMETERS ADAPTATION

The calculation and adjustment of the different types of regulators require knowledge of a sampled parametric model of the system to be regulated. It is therefore necessary to have a tool that makes it possible to obtain, directly from the input and output measurements, the sampled model of the discretized process. Among the identification methods we chose the least squares method [2, 11–15]. It is assumed that the modeled system is linear and has only one input and one output as shown in Fig. 2, the output speed is translated by the following equation [16, 17].

$$A(z^{-1})\omega(k) = z^{-d}B(z^{-1})u(k), \quad (1)$$

with $u(k) = C_{ref}(k) - C_r(k)$,

where $t = k * T_c$, $k \in N_0$, T_c being the sampling period and z^{-1} the unit backward shift operator. In model (1) the polynomials $A(z^{-1})$ and $B(z^{-1})$ take the form:

$$A(z^{-1}) = 1 + a_1z^{-1} + \dots + a_{n_A}z^{-n_A},$$

$$B(z^{-1}) = b_0 + b_1z^{-1} + \dots + b_{n_B}z^{-n_B},$$

provided that $b_0 \neq 0$.

The equation representing the model (1) take other form:

$$\omega(k) = -\sum_{i=1}^{n_A} a_i \omega(k-1) + \sum_{j=0}^{n_B} b_j u(k-d-j) = \Phi^T(k)\theta,$$

with

$$\Phi = [-\omega(k-1) \dots -\omega(k-n_A) \quad u(k-d) \dots u(k-d-n_B)],$$

$$\theta^T = [a_1 \dots a_{n_A} \quad b_0 \dots b_{n_B}].$$

Furthermore $\omega(k)$ is the controlled speed, C_{ref} is the electromagnetic torque reference; C_r is load torque, d is a positive integer representing a delay, the delay d is assumed to be known because it is introduced by the speed control devices.

On the other hand, whatever the estimated parameters are, there is always an error $e(k)$ between the measured actual output speed $\omega(k)$ and the output $\hat{\omega}(k)$ estimated speed by the identification algorithm:

$$e(k) = \omega(k) - \hat{\omega}(k).$$

So the error according to equation (1) is given by:

$$e(k) = \omega(k) - \phi^T(k)\hat{\theta}(k-1)$$

$$= \phi^T(k)[\theta(k) - \hat{\theta}(k-1)].$$

The law of adjustment of the model parameters is given by [2, 13–18]:

$$\hat{\theta}(k) = \hat{\theta}(k-1) + m(k)e(k)$$

$$= \theta(k-1) + m(k)[\omega(k) - \phi^T(k)\hat{\theta}(k-1)], \quad (2)$$

with

$$m(k) = \frac{P(k-1)\phi(k)}{1 + \phi^T(k)P(k-1)\phi(k)}. \quad (3)$$

The covariance matrix $P(k)$ is updated according to:

$$P(k) = \frac{1}{\lambda(k)} [I_{n_p} - m(k)\Phi^T(k)]P(k-1), \quad (4)$$

where I_{n_p} is the $(n_p \times n_p)$ identity matrix and $\lambda(k)$ is the forgetting factor given by:

$$\lambda(k) = 1 - \frac{1 - \Phi^T(k)m(k)}{\sum_0} e^2(k). \quad (5)$$

In (5), \sum_0 is the value imposed to the sum of squares of the a posteriori output prediction errors (residuals), $\hat{\omega}(k)$ the estimated speed at time t by identification loop.

2.2. CALCULATION OF RST PARAMETERS BY PLACEMENT OF POLES

The structure called RST structure consists of the establishment of three polynomials in z^{-1} , $R(z^{-1})$, $S(z^{-1})$, $T(z^{-1})$ as indicated in Fig. 2 [4].

The closed loop transfer function is given by:

$$H_{BF} = \frac{z^{-(d+1)}B(z^{-1})}{A(z^{-1})S(z^{-1}) + z^{-(d+1)}B(z^{-1})R(z^{-1})}. \quad (6)$$

According to the principle of the internal model, the regulator includes an integrator to simplifier, so we put:

$$S(z^{-1}) = 1 - z^{-1} \quad (7)$$

and the polynomial $R(z^{-1})$ written generally by

$$R(z^{-1}) = r_0 + r_1z^{-1} + \dots + r_{n_r}z^{-n_r}. \quad (8)$$

The velocity discrete transfer function is:

$$H_v(z^{-1}) = \frac{b_0}{1 + a_1z^{-1}} z^{-d},$$

with

$(n_A = 1; n_B = 0; d = 1; A(z^{-1}) = 1 + a_1z^{-1}; B(z^{-1}) = b_0)$, and determined the solution of the following diophantine equation:

$$T(z^{-1}) = (1 + \hat{a}_1z^{-1})(1 - z^{-1}) + z^{-d}\hat{b}_0R(z^{-1})$$

$$= (1 - z_1z^{-1})(1 - z_1z^{-1}), \quad (9)$$

\hat{a}_1, \hat{b}_0 are the estimated value of a_1, b_0 by identification

loop and $\deg(T(z^{-1})) = n_p \leq n_A + d$; $\deg(R(z^{-1})) = n_A$.

The equation (9) can be put in a matrix form (Silvestre): $Mx = T$, where M is the square matrix, and the vector contains the polynomial coefficients $R(z^{-1})$. It is desired that the poles be those defined by $T(z^{-1})$ and that the zeros of the system be simplified.

The design of the speed regulator is developed by resorting to the pole assignment technique [9–12]. With the application of such a technique the poles of the closed-loop transfer function are located in any desired locations, defined by the roots of polynomial $T(z^{-1})$, so that the desired characteristics, expressed in terms of closed-loop requirements, are satisfied.

The major points in favor of the pole-assignment technique are that it provides a robust regulator against modeling errors and can cope with no minimum phase systems, the first step in pole-assignment design is to decide the location of closed loop poles.

The second step aims to determine the coefficients of the polynomials $R(z^{-1})$, and $H(z^{-1})$ which define the regulator law.

In equation (9), $z_{1,2}(\rho)$ represent the largest roots of $T(z^{-1})$ given generally by:

$$z_{1,2}(\rho) = e^{-4\rho T_c / T_a} \left[\cos\left(\rho \omega_n T_c \sqrt{1 - \zeta^2}\right) \pm j \sin\left(\rho \omega_n T_c \sqrt{1 - \zeta^2}\right) \right], \quad (10)$$

with $T_a = 4/\zeta\omega_n$, being ω_n the natural frequency, ρ is the pole shifting factor.

Finally, to ensure unitary steady-state gain for the closed-loop transfer function, the simplest choice for $T(z^{-1})$ is: [12, 13]

$$T(z^{-1}) = T_0 = \frac{T(z^{-1})}{\hat{b}_0} \Big|_{z^{-1}=1}.$$

3. CONTROL BY SLIDING MODE OF THE DSI M

The slip mode is a particular function of systems with variable structure. The theory of variable structure systems and slip modes is a nonlinear control technique, characterized by discontinuous controls. The recent interest in this control technique is mainly due to the availability of faster and more powerful microprocessor switches allowing real-time control of dynamic systems [3, 10]. It is a question of first defining a so-called sliding surface which represents the desired dynamics, then synthesizing a control law which ensures the variable to be regulated which slides on this surface and tends towards the origin of the phase plane.

The structure of a sliding mode controller consists of two parts, one concerning the exact linearization U_{eq} and the other stabilizing one with:

$$U = U_{eq} + U_n. \quad (11)$$

U_{eq} is obtained with the equivalent command method [3, 15]. It serves to maintain the variable to be controlled, on the sliding surface $S(x) = 0$, the equivalent command is deduced, considering that the derivative of the surface $\dot{S}(x) = 0$ is zero.

$U_n = 0$ is discontinuous (discrete) control, which allows the system to reach and stay on the sliding surface [10, 15].

The conditions of existence and convergence are the criteria that allow the different dynamics of the system to converge towards the sliding surface and remain independent of the perturbation. Indeed, we present the Lyapunov approach which is to choose a Lyapunov candidate function $V(x) > 0$, (positive scalar function) for the system state variables and to choose a control law that will make to decrease this function $\dot{V}(x) < 0$.

From the direct vector control equations, we derive the following system of equations of states [4, 5, 7]:

$$\begin{cases} \dot{I}_{ds1} = \frac{1}{L_{s1}} [v_{ds1} - R_{s1} I_{ds1} + \omega_s^* (L_{s1} I_{qs1} + T_r \Phi_r^* \omega_{sr}^*)] \\ \dot{I}_{qs1} = \frac{1}{L_{s1}} [v_{qs1} - R_{s1} I_{qs1} - \omega_s^* (L_{s1} I_{ds1} + \Phi_r^*)] \\ \dot{I}_{ds2} = \frac{1}{L_{s2}} [v_{ds2} - R_{s2} I_{ds2} + \omega_s^* (L_{s2} I_{qs2} + T_r \Phi_r^* \omega_{sr}^*)] \\ \dot{I}_{qs2} = \frac{1}{L_{s2}} [v_{qs2} - R_{s2} I_{qs2} - \omega_s^* (L_{s2} I_{ds2} + \Phi_r^*)] \\ \dot{\Phi}_r = -\frac{R_r}{L_m + L_r} \Phi_r + \frac{R_r L_m}{L_m + L_r} (I_{ds1} + I_{ds2}) \\ \dot{\omega} = \frac{1}{j} p \left[\frac{L_m}{L_m + L_r} (I_{qs1} + I_{qs2}) \Phi_r^* - C_r - B_\omega \omega \right], \end{cases} \quad (12)$$

with X^* is the reference value to X and $T_r = \frac{L_r}{R_r}$ is the slip angular frequency is:

$$\omega_s^* = \omega_{sr}^* + \omega_r. \quad (13)$$

$$\begin{cases} \omega_{sr}^* = \frac{R_r}{(L_m + L_r)} (I_{qs1}^* + I_{qs2}^*) \\ \Phi_r^* = L_m (I_{ds1}^* + I_{ds2}^*) \\ C_{em}^* = p \frac{L_m}{L_m + L_r} \Phi_r^* (I_{qs1}^* + I_{qs2}^*) \end{cases} \quad (14)$$

The regulating surface of the flow is of the following form:

$$\begin{cases} S(\Phi) = \Phi_r^* - \Phi_r \\ I_{ds} = I_{dsn} + I_{dseq} \end{cases}, \quad (15)$$

$$\dot{S}(\Phi) = \dot{\Phi}_r^* + \frac{R_r}{L_m + L_r} \Phi_r - \frac{R_r L_m}{L_m + L_r} I_{dseq} - \frac{R_r L_m}{L_m + L_r} I_{dsn}. \quad (16)$$

During the sliding mode and the steady state, we have $S(\Phi)=0$ and consequently $\dot{S}(\Phi)=0$ and $I_{qsn}=0$ we draw the formula of the equivalent command I_{dseq} from (16).

$$\begin{cases} I_{dseq} = \frac{L_m + L_r}{R_r L_m} \left[\dot{\Phi}_r^* + \frac{R_r}{L_m + L_r} \Phi_r \right] \\ I_{dsn} = K_\Phi \frac{S(\Phi)}{|S(\Phi) + \varepsilon_\Phi|} \end{cases} \quad (17)$$

To adjust the currents the surfaces of the currents are laid as follows:

$$\begin{cases} S(I_{ds1}) = I_{ds1}^* - I_{ds1} \\ S(I_{ds2}) = I_{ds2}^* - I_{ds2} \\ S(I_{qs1}) = I_{qs1}^* - I_{qs1} \\ S(I_{qs2}) = I_{qs2}^* - I_{qs2} \end{cases} \quad (18)$$

and the reference voltages are:

$$\begin{cases} v_{ds1}^* = v_{ds1} + v_{ds1eq} \\ v_{ds2}^* = v_{ds2} + v_{ds2eq} \\ v_{qs1}^* = v_{qs1n} + v_{qs2eq} \\ v_{qs2}^* = v_{qs2n} + v_{qs2eq} \end{cases} \quad (19)$$

After replacing the voltages by the reference voltages, we find

$$\begin{cases} \dot{S}(I_{ds1}) = \dot{I}_{ds1}^* - \dot{I}_{ds1} \\ \dot{S}(I_{ds2}) = \dot{I}_{ds2}^* - \dot{I}_{ds2} \\ \dot{S}(I_{qs1}) = \dot{I}_{qs1}^* - \dot{I}_{qs1} \\ \dot{S}(I_{qs2}) = \dot{I}_{qs2}^* - \dot{I}_{qs2} \end{cases} \quad (20)$$

During slip mode and steady state, we have:

$$\begin{cases} S(I_{ds1}) = 0 \Rightarrow \dot{S}(I_{ds1}) = 0 & \text{and} & v_{ds1n} = 0 \\ S(I_{qs1}) = 0 \Rightarrow \dot{S}(I_{qs1}) = 0 & \text{and} & v_{qs1n} = 0 \\ S(I_{ds2}) = 0 \Rightarrow \dot{S}(I_{ds2}) = 0 & \text{and} & v_{ds2n} = 0 \\ S(I_{qs2}) = 0 \Rightarrow \dot{S}(I_{qs2}) = 0 & \text{and} & v_{qs2n} = 0 \end{cases} \quad (21)$$

So, we draw from the equations (19), (20) and (21), expressions of equivalent commands:

$$\begin{cases} v_{ds1eq} = L_{s1} \dot{I}_{ds1}^* + R_{s1} I_{ds1} - [L_{s1} I_{qs1} + T_r \Phi_r^* \omega_{sr}^*] \\ v_{qs1eq} = L_{s1} \dot{I}_{qs1}^* + R_{s1} I_{qs1} - \omega_s^* [L_{s1} I_{ds1} + \Phi_r^*] \\ v_{ds2eq} = L_{s2} \dot{I}_{ds2}^* + R_{s2} I_{ds2} - \omega_s^* [L_{s2} I_{qs2} + T_r \Phi_r^* \omega_{sr}^*] \\ v_{qs2eq} = L_{s2} \dot{I}_{qs2}^* + R_{s2} I_{qs2} - \omega_s^* [L_{s2} I_{ds2} + \Phi_r^*] \end{cases} \quad (22)$$

We take:

$$\begin{cases} v_{ds1n} = K_{d1} \frac{S(I_{ds1})}{|S(I_{ds1})| + \zeta_{d1}} \\ v_{qs1n} = K_{q1} \frac{S(I_{qs1})}{|S(I_{qs1})| + \zeta_{q1}} \\ v_{ds2n} = K_{d2} \frac{S(I_{ds2})}{|S(I_{ds2})| + \zeta_{d2}} \\ v_{qs2n} = K_{q2} \frac{S(I_{qs2})}{|S(I_{qs2})| + \zeta_{q2}} \end{cases} \quad (23)$$

During the convergence mode, Lyapunov stability conditions are checked.

The rotor flux are estimated by the following two equations:[3, 17 – 20].

$$\begin{cases} \frac{d\hat{\Phi}_{dr}}{dt} = \frac{R_r L_m}{L_m + L_r} (I_{ds1} + I_{ds2}) + \omega_s^* \hat{\Phi}_{qr} - \frac{R_r}{L_m + L_r} \hat{\Phi}_{dr} \\ \frac{d\hat{\Phi}_{qr}}{dt} = \frac{R_r L_m}{L_m + L_r} (I_{qs1} + I_{qs2}) - \omega_s^* \hat{\Phi}_{dr} - \frac{R_r}{L_m + L_r} \hat{\Phi}_{qr} \end{cases} \quad (24)$$

The rotor flux module is calculated as follows:

$$\hat{\Phi}_r = \sqrt{\hat{\Phi}_{dr}^2 + \hat{\Phi}_{qr}^2} \quad (25)$$

4. SIMULATION AND INTERPRETATION OF RESULTS

Figure 2 shows the global schema to control adaptive of DSIM speed by sliding mode, followed by the application of the load $C_r = 14$ Nm and -14 Nm respectively between the time intervals $t = [1, 2]$ and $[2.25, 4]$ s, imposing the reference speed $N = 2500$ rpm. The sliding regulator parameters chosen by:

Table 1
Sliding regulator parameters

Area	$S(\Phi)$	$S(I_{ds1})$	$S(I_{qs1})$	$S(I_{ds2})$	$S(I_{qs2})$
K	120	120	150	150	150
ζ	0.95	0.95	0.95	0.95	0.95

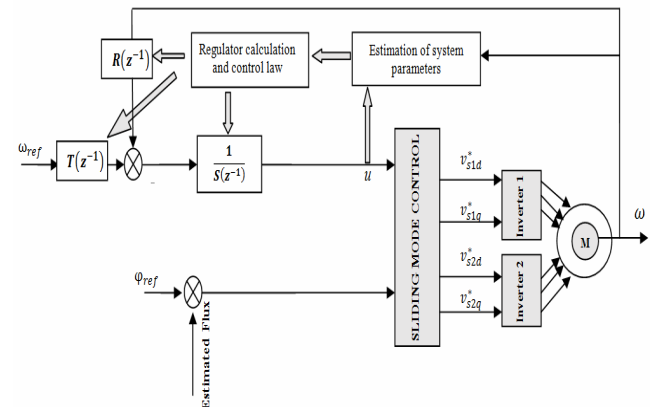


Fig. 2 – Adaptive speed control scheme of the DSIM by sliding mode.

The initial value of identification by least squares: $\theta(0)=[0 \ 0.01]$ and initial covariance matrix $P(0)=2000I_2$, $\Sigma_0=10^{-2}$ and the two largest roots of polynomial $T(z^{-1})$ are characterized by $\zeta = 0.7$, $\omega_n = 114$, leading to $T_a = 50$ ms and flux is imposed $\Phi_r^* = 1$ Wb, while the fastest two are real, the value of these roots is obtained letting $\rho = 1$. This shows in Fig. 3: at startup and during the transient regime, the speed increases linearly with time, and it reaches its reference value at $t = 0.45$ s without exceeding. The electromagnetic torque reaches the maximum value of 54 N.m at $t = 0.014$ s, then it reaches the steady state at $t = 0.45$ s without exceeding. At the beginning, the stator currents $i_{as1} = i_{as2} = 22.4$ A that is, they have a inrush current of about 4 times the rated current, hence from $t = 0.31$ s they decrease in an almost linear fashion up to $t = 0.42$ s.

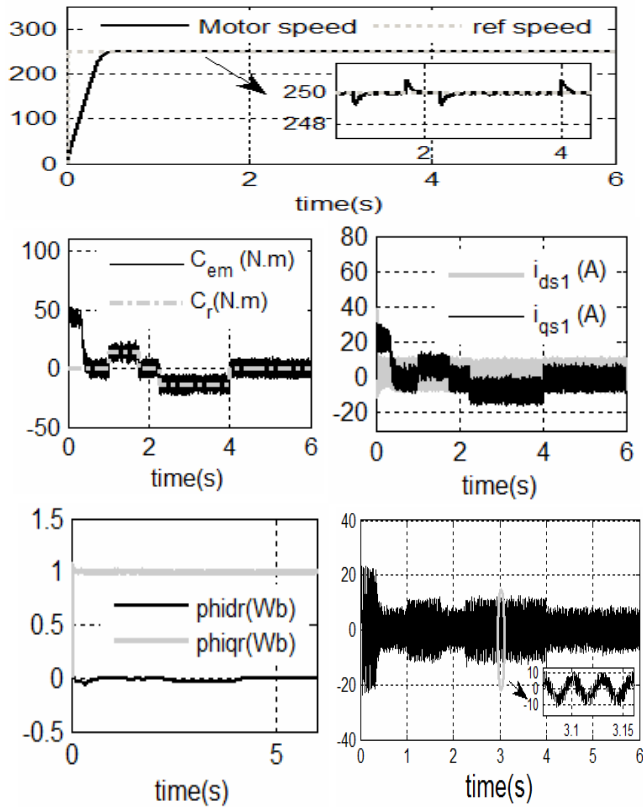


Fig. 3 – Simulation of the speed control of the DSIM with the application of the variation resistant torque at $t = [1, 1.75]$ and $[2.25, 3]$ s.

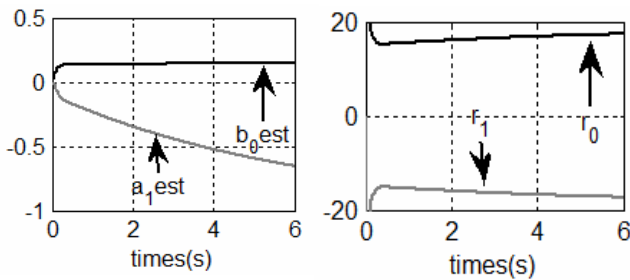


Fig. 4 – The values of estimated parameters of a_1 , b_0 and regulator parameters r_0 , r_1 .

The current in quadrature, initially reached 25 A, near it evolves identically to the electromagnetic torque, the rotor flows according to (d, q) at the start of peaks during a fraction of a second oscillating around their instructions, then they stabilize at $t = 0.31$ s and continue their journey according to their references. The parameters of model a_1, b_1 and regulating r_0, r_1 are insensitive at the time of load variation (Fig. 4).

5. TESTS OF ROBUSTNESS

We reverse the speed from 2500 to -2500 rpm from time $t = 1.5$ s. The results clearly show in Fig. 5 during the transient regime and before the reversal of the speed (from $t = 0$ s to 1.5 s), the gaits evolve in a manner identical to that observed previously, but from $t = 1.5$ s, the speed inverse and reached its negative set point after $t = 0.75$ s without any overruns. This generates, an increase in the current i_{as1} (A) of a magnitude equal to that recorded during the start, which stabilizes after 0.75 s, to restore the shape of the steady state, the electromagnetic torque reaches $(-50$ N.m) at the moment of the reversal of the speed, which stabilizes as soon as the latter reaches its negative set point value $(-2500$ rpm), the rotor flux curves observe a slight variation during the reversal of the speed.

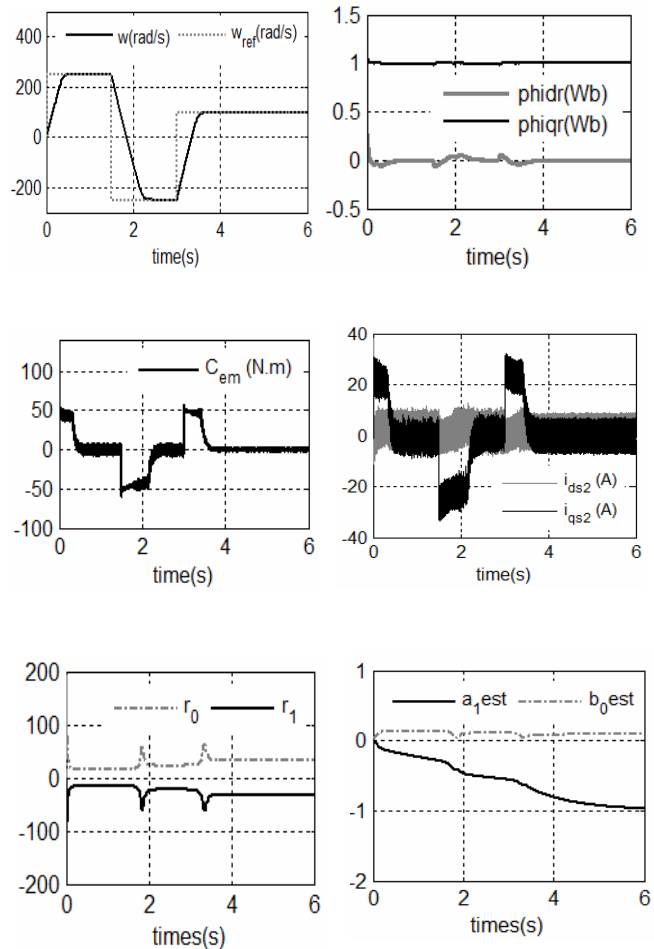


Fig. 5 – Robustness of the speed control of DSIM in the presence of set point variation $[250; -250; 100]$ rad/s.

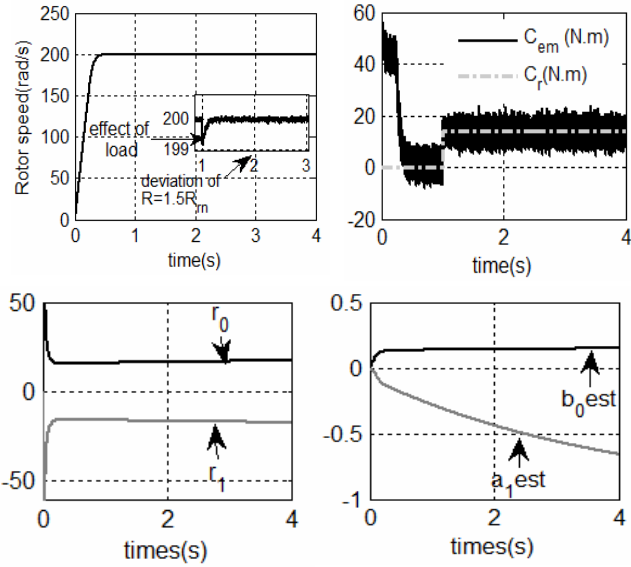


Fig. 6 – Simulated results test of robustness for load torque $C_r = 14\text{N.m}$ at $t = 1\text{ s}$ and deviation of value rotor resistance at $t = 2\text{ s}$.

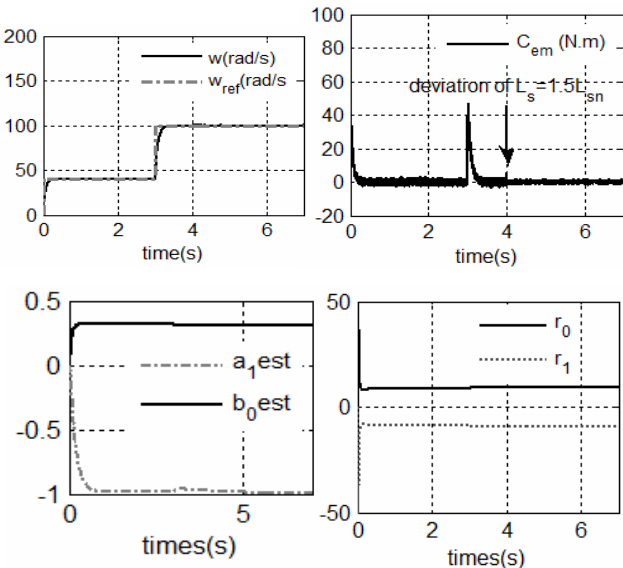


Fig. 7 – Simulated results test of robustness for starting DSIM in low speed and deviation of value of $(L_s = 2L_{sn})$ at $t = 4\text{ s}$.

The robustness test shows in Fig. 6 validate the insensitivity of the speed control by the robust RST regulator to the parametric variations due to the increase of R_r at $t = 2\text{ s}$ of the machine.

The simulation results in Figs. 5, 6 and 7 can ensure robustness against uncertainties of mechanical and electrical parameters of the motor by the insensitivity of parameters variation (R_r, L_s , speed variation, load variation), it also correct performances of the controller in term of stability and performance.

6. CONCLUSION

In order to improve the speed adjustment, the sliding mode adaptive control technique based on the reference model has been applied. The adaptation of the RST controller parameters over time by the closed loop output

error algorithm makes the control of the DSIM robust with respect to variations in the parameters of the machine. The simulation results clearly show that the self-tuning speed of the DSIM is robust and satisfactory in terms of speed and tracking of the reference speed (response time and time for speed reversal), the absence of peaks at the electromagnetic torque level is noted, and the disturbance (load) rejection time is low when an external (load) perturbation is applied. The tests of robustness with respect to the variations parameters (rotor resistance, inductance, speed inverse, startup low speed) show that the robust adaptive regulation gives good responses of speed, of electromagnetic torque. It can be concluded that the applied control is robust and efficient during normal operation or under severe operating conditions.

Finally, the experimental implementation of the proposed control scheme will be addressed in the future work.

Table 2

The used DSIM parameters [1–3]

Parameter name	Symbol	Value	Unit
DSIM Mechanical power	P_n	4.5	kW
Nominal tension	V_n	220	V
Nominal Currants	I_n	5.6	A
Nominal speed	N	2970	rpm
Stator resistances	$R_{s1} = R_{s2} = R_s$	3.72	Ω
Rotor resistance	R_r	3.72	Ω
Stator self inductances	$L_{s1} = L_{s2} = L_s$	0.022	H
Rotor self inductance	L_r	0.006	H
Mutual inductance	L_m	0.3672	H
Moment of inertia	j	0.0662	kg.m ²
Viscous friction coefficient	B_ω	0.001	N.m/rad
Supply frequency	f	50	Hz
Pole pairs number	P	1	/

Received on July 31, 2018

REFERENCES

1. D. Hadiouche, H. Razik, A.Rezzoug, *Study and simulation of space vector PWM control of double star induction motors*, Power Electronics Congress, International, pp. 42–47 (2000).
2. I.D. Landau, A. Karimi, *Recursive algorithms for identification in closed loop a unified approach and evaluation*, Automatica, **33**, 8, pp. 1499–1523 (1997).
3. H. Amimeur, R. Abdessemed, D. Aouzellag, *A sliding mode control Associated to the field oriented control of dual stator induction motor drives*, Revue des Energies Renouvelables, **11**, 2, pp. 317–327 (2008).
4. N. Akkari, A. Chaghi, R. Abdessemed, *Study and simulation of RST regulator applied to a double fed induction machine (DFIM)*, Journal of Electrical Engineering & Technology, **3**, 3, pp. 308–313 (2008).
5. J.L. Chang, *Dynamic sliding mode controller design for reducing chattering*, Journal of the Chinese Institute of Engineers, **37**, 1, pp. 71–78 (2005).
6. C.Y. Chan, *Discrete adaptive sliding mode control of a class of stochastic system*, Automatică, **35**, 19, pp. 1491–1498 (1999).
7. S. Lekhchine, T. Bahi, *Indirect rotor field oriented control based on fuzzy logic controlled double star induction machine*, International Journal of Electrical Power and Energy Systems, **57**, 4, pp. 206–211 (2014).
8. L. Sheng, G. Xiaojie, Z. Lanyong, *Robust Adaptive Backstepping Sliding Mode Control for Six-Phase Permanent Magnet*

- Synchronous Motor Using Recurrent Wavelet Fuzzy Neural Network*, IEEE Access, **5**, 1, pp. 14502–14515 (2017).
9. G. Fusco, M. Russo, *Adaptive voltage regulator design for synchronous generator*, IEEE Transactions on Energy Conversion, **23**, 3, pp. 946–956 (2008).
 10. K. Jamoussi, Ch. Alaoui, M. Ouali, *Robust Sliding Mode Control Using Adaptive Switching Gain for Induction Motors*, International Journal of Automation and Computing, **10**, 4, pp. 303–911 (2013).
 11. G. Fusco, M. Russo, *Self-tuning regulator design for nodal voltage waveform control in electrical power systems*, IEEE Transactions on Control Systems Technology, **11**, 2, pp. 258–266 (2003).
 12. G. Fusco, M. Russo, *Nodal voltage regulation employing an indirect self-tuning approach*, In: Proceedings of the IEEE Conference on Control Applications, Toronto Canada, August, **28**, 31, pp. 797–802, 2015.
 13. I. Landau, *From robust control to adaptive control*, Control Engineering Practice, **7**, 9, pp. 1113–1124 (1999).
 14. A. Levant, *Sliding order and sliding accuracy in sliding mode control*, International Journal of Control, **58**, 6, pp. 1247–1263, 1993.
 15. V. Utkin, *Sliding mode control design principles and applications to electric drives*, IEEE Transactions on Industrial Electronics, **40**, 1, pp. 23–37 (1993).
 16. H. Du, Y. Xinghuo, *Chattering free discrete time sliding mode control*, Automatica, **68**, 2, pp. 87–91 (2016).
 17. J. Lin Chang, *Dynamic sliding mode controller design for reducing chattering*, Journal of the Chinese Institute of Engineers, **37**, 1, pp. 71–78 (2014).
 18. Y. Chan, *Discrete adaptive sliding-mode control of a class of stochastic systems*, Automatică, **35**, 19, pp. 1491–1498 (1999).
 19. L. Cristian, B. Frede, *Super twisting sliding mode direct torque control of induction machine drives*, In: IEEE Energy Conversion Congress and Exposition (ECCE), pp. 5116–5122, USA, 2014.
 20. W. Wencen, *An adaptive Luenberger observer for speed sensorless estimation of induction machines*, Annual American Control Conference (ACC), Milwaukee, WI, USA, pp. 307–312, 2018.